International Journal of Pharmaceutics 421 (2011) 397–404

Contents lists available at SciVerse ScienceDirect

International Journal of Pharmaceutics

journal homepage: www.elsevier.com/locate/ijpharm

Heparin-coated superparamagnetic nanoparticle-mediated adeno-associated virus delivery for enhancing cellular transduction

Jun-Ho Hwang, Slgirim Lee, Eunmi Kim, Jung-Suk Kim, Chang-Ha Lee, Ik-Sung Ahn, Jae-Hyung Jang*

Department of Chemical and Biomolecular Engineering, Yonsei University, Seoul 120-749, Republic of Korea

ARTICLE INFO

Article history:
Received 27 July 2011
Received in revised form 5 October 2011
Accepted 7 October 2011
Available online 13 October 2011

Keywords:
Heparin
Adeno-associated virus
Iron oxide nanoparticle
Magnetism

ABSTRACT

Superparamagnetic iron oxide nanoparticles (SPIONs) have been exploited as an elegant vehicle to enhance gene delivery efficiencies in gene therapy applications. We developed a magnetically guided adeno-associated virus (AAV) delivery system for enhancing gene delivery to HEK293T and PC12 cell lines. Wild-type AAV2 and a novel AAV vector, AAVr3.45, which was directly evolved in a previous study to possess diverse cell tropisms, were used as gene carriers. Additionally, the affinity of each viral vector to heparin was employed as a moiety to immobilize virus onto heparin-coated SPIONs (HpNPs). Magnetically guided AAV delivery resulted fast and efficient cellular transduction. Importantly, a short exposure of virus to target cells under a magnetic field (<180 min) yielded comparable transduction produced by the conventional gene-delivery protocol (i.e., 24 h-incubation of virus with target cells prior to replacing with fresh medium). Additionally, magnetic guidance of AAV encoding nerve growth factor (NGF) produced sufficient functional NGF, leading to robust neurite elongation by PC12 as compared to direct NGF protein delivery or non-magnetic delivery. The successful establishment of a magnetically guided AAV delivery system, with the ability to efficiently and rapidly infect target cells, will provide a powerful platform for a variety of gene therapy applications.

1. Introduction

Virus-mediated gene delivery has emerged as a powerful strategy for the treatment of a variety of human diseases, including Parkinson's disease (Kaplitt et al., 1994), X-linked adrenoleukodystrophy (Cartier et al., 2009), hemophilia B (Kay et al., 2000), and Leber's congenital amaurosis (Maguire et al., 2009), due to the greater gene transfer efficiencies of viral vectors than non-viral vectors. However, a number of challenges associated with viral gene delivery, such as the innate immunogenicity of viral vectors, limited tropism, spread of vectors to distant sites, and inefficient delivery to non-permissive cell types (Smith-Arica et al., 2003; Selkirk, 2004), have continuously emphasized the need for significant advancements in developing safe and efficient virus delivery systems.

Superparamagnetic iron oxide nanoparticles (SPIONs), which exhibit magnetization only in an applied magnetic field, have been recently exploited as an elegant vehicle to enhance gene delivery efficiencies in gene therapy applications (Dobson, 2006). In this approach, gene delivery vectors are linked to the SPIONs, which are then introduced into target cells by an external magnetic field generated by magnets placed below the culture plates. A magnetic force drives the SPIONs associated with gene vectors into the cellular microenvironment, maintaining locally elevated concentrations at the cellular membrane for a short period of time. The key features of SPION-mediated gene delivery include enormously reduced vector exposure time to cells for yielding sufficient gene expression and significantly enhanced gene delivery efficiencies, even in non-permissive cell types (Dobson, 2006; Lin et al., 2008).

In this study, the synergistic effect of viral gene delivery using SPION for enhancing gene delivery efficiencies has been investigated by tagging adeno-associated viral (AAV) vectors onto heparin-coated iron oxide superparamagnetic nanoparticles (HpNPs) (Fig. 1). AAV has been broadly explored in clinical trials due to its safety and efficiency as a gene delivery vector. AAV is a parvovirus with a 4.7 kb single-stranded DNA genome containing two genes (*rep* and *cap*). AAV infection results in persistent latent infection in a broad range of both dividing and non-dividing cells (Kaplitt et al., 1994; Fisher et al., 1997; Flannery et al., 1997). The affinity of AAV to heparin, which is structurally similar to the heparan sulfate proteoglycan (HSPG) that is a primary receptor for AAV2, has been employed to immobilize AAV vectors onto the HpNPs. In our study, magnetically guided AAV delivery resulted in significantly reduced viral exposure time to induce similar or enhanced cellular transduction compared to the delivery of freely dispersed AAV vectors. The enhanced cellular transduction by magnetic guidance was primarily caused by the direct penetration of viral vectors through physical

* Corresponding author. Tel.: +82 2 2123 2756; fax: +82 2 312 6401.
E-mail address: j-jang@yonsei.ac.kr (J.-H. Jang).

0378-5173/$ – see front matter © 2011 Elsevier B.V. All rights reserved.
doi:10.1016/j.ijpharm.2011.10.019

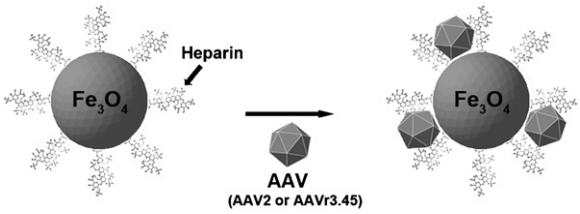

Fig. 1. Schematic illustration of magnetically guided AAV/HpNP complexes: (A) heparin-coated superparamagnetic iron oxide nanoparticles (HpNPs) and (B) AAV bound HpNPs.

forces (i.e., under a magnetic field) (Haim et al., 2005; Kamei et al., 2009; Orlando et al., 2010; Kim et al., 2011). Additionally, the level of transgene expression driven by the magnetically guided delivery was sufficient to induce physiological responses, such as neurite extension, thereby demonstrating the great potential of magnetically driven viral delivery for a variety of gene therapy applications.

2. Materials and methods

2.1. Heparin-coated superparamagnetic iron oxide nanoparticles (HpNPs)

Heparin-coated superparamagnetic iron oxide nanoparticles (SPIONs: fluidMAG-Heparin) were purchased from Chemicell (Berlin, Germany). According to the manufacturer's guidance, hydrodynamic diameter of the SPION is approximately 100 nm, and a highly sulfated glycosaminoglycan, heparin, is conjugated to the nanoparticles. The HpNPs were diluted in aqueous solution containing 40 mM NaCl prior to viral binding.

2.2. Cell culture

AAV 293 cells (Stratagene, La Jolla, CA) were utilized for viral packaging and cultured in Dubach's modified Eagle medium (DMEM; Invitrogen, Carlsbad, CA) with 10% fetal bovine serum (FBS) (Invitrogen) and 1% penicillin/streptomycin (Invitrogen) at 37 °C and 5% CO_2. HEK293T and PC12 were cultured for analyzing transduction efficiencies. HEK293T cells were grown under the same conditions as AAV 293 cells. The PC12 cell line, which is derived from a pheochromocytoma of the rat adrenal medulla, was cultured in RPMI (Royal Park Memorial Institute) medium (Invitrogen) with 10% FBS, 7.5% horse serum (Invitrogen), and 1% penicillin/streptomycin at 37 °C and 5% CO_2.

2.3. Production and purification of AAV vectors

Two AAV vectors were packaged and utilized as gene carriers in this study: (i) wild-type AAV2 and (ii) a novel AAV vector, AAVr3.45, which was newly generated through directed evolution specifically for infecting various non-permissive cell types in a previous study (Jang et al., 2011). AAVr3.45 carried an insertion of LATQVGQKTA (wt AAV2: ^{583}LQRGNRQA-), where LA and A are linker residues, at amino acid (aa) 587 with an additional V719M mutation (Jang et al., 2011). Recombinant AAV2 and AAV r3.45 vectors, carrying cDNA encoding green fluorescence protein (GFP) driven by a cytomegalovirus (CMV) promoter, were packaged using the transient transfection method. Briefly, an equal mass (17 μg) of three plasmids, including an AAV helper plasmid (pXX2 for AAV2 and pAAV r3.45 carrying a *cap r3.45* for AAVr3.45), CMV GFP vector plasmid containing ITR (pAAV CMV GFP SN), and an adenoviral helper plasmid (Stratagene), were transfected via calcium phosphate into AAV 293 cells (Maheshri et al., 2006). The resulting viral vectors were harvested as previously described (Koerber et al., 2006) and purified using heparin column chromatography (Zolotukhin et al., 1999). Briefly, each crude lysate (i.e., AAV2 and AAV r3.45) was loaded onto a 1 mL HiTrap heparin column (GE Healthcare, Pittsburgh, PA), which was previously equilibrated with Tris buffer (50 mM, pH 7.5) containing 150 mM NaCl. The column was washed with 3 mL of 150 mM NaCl, and elutions were performed with 3 mL of 1 M NaCl. The viral fractions were desalted and buffer exchanged into phosphate-buffered saline (PBS)/0.01% Tween20 using Amicon Ultra-15 Centrifugal Filter Units (Millipore, Billerica, MA) according to the manufacturer's instructions. DNase-resistant genomic titers were determined by quantitative PCR (QPCR; Mini Opticon, Bio-Rad, Hercules, CA).

2.4. Preparation of AAV/heparin-coated iron oxide nanoparticles

The AAV vectors (4×10^8 viral genomic particles for HEK293T infection, 4×10^9 viral genomic particles for PC12 infection), including AAV r3.45 and AAV2, were diluted in 50 μL of serum-free DMEM and mixed with the HpNPs suspended in 50 μL of serum-free DMEM with different HpNP quantities (i.e., 0.005, 0.05, 0.5, 5, or 10 μg). The mixture was vigorously mixed for 5 min at room temperature, and then an additional 200 μL of serum-free DMEM was immediately added to reduce the aggregation of AAV-HpNP complexes. To examine the association of AAV vectors with the HPNP, after 1 h of magnetic sedimentation (NeoDeltaMagnet; 1170–1250 mT, IBS magnet, Berlin, Germany), the genomic particles of unbound AAV vectors in the supernatant were determined by quantitative PCR (QPCR).

2.5. Transduction assay

Hydrodynamic particle sizes of AAV/HpNP complexes were determined by dynamic light scattering using a Zetasizer (Zen3600, Malvern Instruments Ltd., Worcestershire, United Kingdom). Additionally, the immobilization of AAV onto the heparin-coated SPIONs was visualized using transmission electron microscopy (TEM) (JEM-2011, JEOL Ltd., Tokyo, Japan) at the Yonsei Center for Research Facilities. TEM images were undertaken at 200 kV with 400,000× magnification.

2.6. Transduction assay

To test the infectivity of HpNP-mediated AAV delivery, the AAV/HpNP complexes carrying cDNA coding GFP driven by the CMV promoter (viral genomic multiplicity of infection (MOI): 10^4 (HEK293T) and 10^5 (PC12)) were added on top of the medium containing cells (HEK293T and PC12; 4×10^4 cells/well) grown in 24-well tissue culture plates (TCP) in the presence or absence of a magnetic field (MagnetoFACTOR Plate 24, Chemicell, Berlin, Germany). Each cell was exposed to the magnetic field (130 mT) for 5, 30 or 180 min. Cell culture media containing AAV/HpNP or AAV vectors was replaced with fresh media at each time point. The percentage of GFP expressing cells out of the total number of cells was determined at 48-h post-infection using flow cytometry at Yonsei University College of Medicine Medical Research Center (Becton Dickinson FACS Caliber, Becton-Dickinson, Sunnyvale, CA).

2.7. Internalization of AAV-nanoparticles into cytoplasm

AAV vectors, which were bound to the HpNPs, were fluorescently labeled with Alexa Fluor 594 using a microscale protein labeling kit (Invitrogen), and the internalization of AAV vectors was visualized by imaging fluorescently labeled AAV vectors within the cytoplasm (Eclipse Ti-S, Nikon, Tokyo, Japan). To remove surface-associated viral vectors, the cells infected by the magnetically driven AAV vectors were trypsinized immediately after being

exposed to AAV/HpNP complexes for 5, 30, or 180 min, re-plated onto new 24-well TCPs, grown for additional 12 h prior to visualizing the internalized AAV vectors to access the capability of rapid internalization via HpNP-mediated AAV delivery under magnetic forces versus the delivery of freely dispersed virus (i.e., virus only) or HpNP-mediated delivery without magnetic forces.

2.8. Cell viability

To analyze the viability of cells infected by the AAV2/HpNP complexes, metabolically active cells were stained with 3-(4,5-dimethylthiazol-2-yl)-2,5-diphenyltetrazolium bromide (MTT; Sigma–Aldrich) and colorimetric changes were quantified at 550 nm using a spectrophotometer (Nanodrop 2000; Thermo Scientific, West Palm Beach, FL) compared with the ones measured for a negative control (i.e., no infection). Each cell (HEK293T, PC12) was infected by AAV2 only or AAV2/HpNP complexes with or without magnetic forces and harvested after 48 h. Cell viabilities were determined using only AAV2. Briefly, an MTT solution (20 μL of 2.5 μg/μL in 200 μL medium) was dispensed into each well, and the cultures were incubated for 4 h at 37 °C. Supernatants were collected and mixed with dimethyl sulfoxide (DMSO; EMD Biosciences, Gibbstown, NJ), and spectrophotometric absorbances (550 nm) were measured using a NanoDrop 2000 (Thermo Scientific, West Palm Beach, FL). Finally, the absorbance values were normalized to the absorbance value of the negative control, in which cells were cultured without viral infection for the same durations.

2.9. Neurite extension

The quantification of neurite outgrowth from PC12 cells was conducted to examine physiological levels of nerve growth factors (NGF) produced by HpNP-mediated AAV delivery. Delivery of mouse β-NGF protein (100 ng/mL) (ProSpec-TanyTechnogene, Ltd., East Brunswick, NJ, USA) was utilized as a positive control. To construct a plasmid encoding NGF driven by the CMV promoter, the full-length mouse NGF in the RK5 vector backbone (pNGF), which was a gift from Dr. Shea (Northwestern University, USA), was digested with *Sal*I and *Not*I, and the products ligated to create the recombinant AAV packaging plasmid pAAV CMV NGF. The resulting AAV2 and AAVr3.45 vectors carrying NGF (genomic MOI 10^5: 4×10^9 genomic particles) were complexed with 10 μg of HpNPs and incubated with PC12 under magnetic forces for 5, 30, or 180 min. After 48 h, cells were stained using fluorescein diacetate (Sigma) dissolved in PBS (8 μg/mL; final concentration) for easy recognition of neurite extensions, and the total neurite length per field was quantified using the tracing algorithm in the Neuron J plug-in for ImageJ (Meijering et al., 2004). Fifteen fields of views per condition (five images per field, $n = 3$) were averaged to determine neurite extension.

2.10. Statistical analysis

All of the experiments were performed in triplicate, and the experimental data were expressed as mean ± standard deviation (SD). All of the data were analyzed by one-way analysis of variance (ANOVA) with a *post hoc* Dunnett test using the SPSS 18.0 software package (IBM Corporation, Somers, NY, USA).

3. Results and discussion

3.1. Characterization of AAV/HpNP complexes

The affinity of AAV to heparin was employed to immobilize each viral vector (i.e., AAV2 and AAV r3.45) onto the heparin-coated

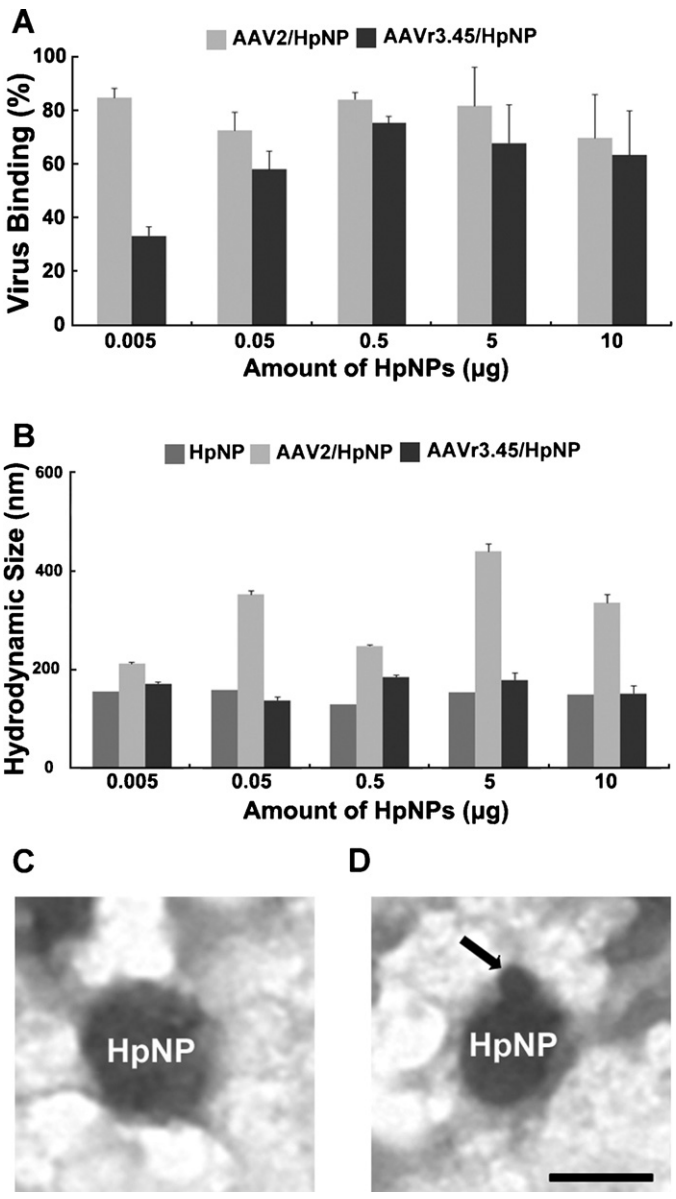

Fig. 2. Characterization of HpNPs, AAV2 and AAV r3.45/HpNP complexes: (A) HpNP-bound quantity of AAV2 and AAVr3.45 as a function of the amount of HpNPs, (B) hydrodynamic particle sizes of HpNPs only, AAV2/HpNPs, and AAVr3.45/HpNPs determined by dynamic light scattering, and representative transmission electron microscope (TEM) images of HpNP only (C) and AAV2-bound HpNP particle (D). Values are reported as mean ± standard deviation (SD). The scale bar indicates 100 nm.

superparamagnetic iron oxide nanoparticles (HpNPs), as schematically illustrated in Fig. 1. AAV r3.45, generated through directed evolution, is the vector that demonstrated the greatest transduction efficiency in various non-permissive cell types, including neural stem cells, fibroblasts, and HeLa cells (Jang et al., 2011). Heparin is structurally similar to heparan sulfate proteoglycan (HSPG), which is a primary receptor for AAV2 (Zolotukhin et al., 1999); therefore, we used heparin as a moiety to immobilize virus onto the HpNPs. Genomic titers of AAV r3.45 vectors, produced by the transient transfection method followed by heparin column purification, were slightly higher (1.1×10^{13} vg (viral genomes)/mL) than those of the wild type AAV2 (6.8×10^{12} vg/mL) generated by the same method. Wild-type AAV2 exhibited greater binding ability to HpNPs (72.6–84.9%) than AAV r3.45 (33.2–75.4%), implying a somewhat lower heparin affinity of AAV r3.45 (Fig. 2A). The percentage of binding ability indicates the viral genomic particles bound to the

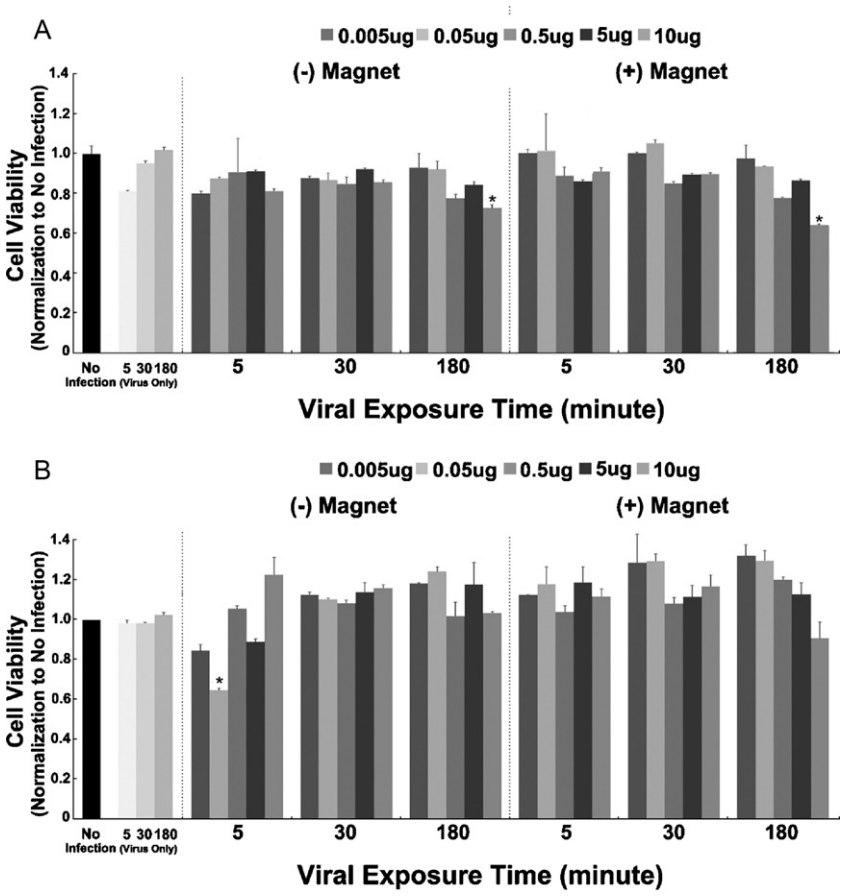

Fig. 3. Cell viabilities of HEK293T cells (A) and PC12 cells (B) upon no infection, exposure to AAVr3.45 only (5, 30, or 180 min without magnetic forces), and exposure to AAV r3.45/HpNPs with or without magnetic forces. The MTT assay was performed to measure the metabolic activities of HEK293T (A) and PC12 cells (B) treated with AAVr3.45 formulated with different quantities of HpNPs (0.005, 0.05, 0.5, 5, or 10 μg) under various viral exposure times (5, 30, or 180 min). Values are reported as mean ± SD. The symbol * indicates statistically significant differences between the cells treated with the designated conditions and the cells treated with no infection ($P < 0.05$).

HpNPs relative to the initial viral quantities used prior to viral binding to HpNPs. This lower affinity could be due to a considerable functional alteration around the heparin binding domain on the AAVr3.45 capsid. AAV r3.45 carries an insertion of LATQVGQKTA (where LA and A are linker residues) at aa 587 with an additional V719M mutation. The inserted peptide likely lies on the surface of the threefold spike within the heparin-binding site; thus, the heparin affinity of AAV r3.45 might be slightly altered as compared with wild-type AAV2 (Jang et al., 2011). While the binding quantity of AAV2 on the HpNPs maintained consistency upon interactions with different HpNPs (0.005, 0.05, 0.5, 5, or 10 μg), the quantity of AAV r3.45 on the HpNPs increased from 33.2% to 75.4% as the mass of HpNP increased up to 0.5 μg. Because the majority of AAV vectors (AAV2, AAV r3.45) successfully bound to the HpNPs, the separation of unbound-AAV vectors prior to infection was not necessary.

The hydrodynamic sizes (number-weighted) of the AAV/HpNPs complexes varied depending on the vector type. The sizes of the HpNP complexes formed with AAV2 increased approximately 2–4-fold (213.6–441.2 nm) as compared to the HpNPs only (~100 nm). However, those HpNPs formulated with AAV r3.45 (139.2–187.3 nm) were slightly increased compared with HpNPs only (Fig. 2B). While the particle sizes of AAVr3.45/HpNPs seemed independent of the quantity of nanoparticles, those of AAV2/HpNPs were mostly increased as the mass of nanoparticles increased, except for complexes with 0.5 μg HpNPs. The higher affinity of AAV2 to heparin may result in more extensive interactions of AAV2 with heparins coated on the nanoparticles than AAV r3.45, possibly causing particle aggregation. The spherical morphologies of the HpNPs and the immobilization of AAV r3.45 on the HpNPs were visualized using transmission electron microscopy (TEM) (Fig. 2C and D). HpNPs with approximately 100 nm diameters and the display of small particles (arrow), presumably AAV vectors, on the HpNPs were observed. This result confirms the successful binding of AAV vectors with HpNPs prior to cellular transduction.

3.2. Cell viability

The effect of HpNP-mediated AAV delivery under magnetic forces on the metabolic functions of cells (HEK293T and PC12 cells) was examined by comparing magnetically treated cells cultured without magnetic forces or without viral infections. Note that only the effects of AAV r3.45/HpNP delivery on viabilities of HEK293T and PC12 cells were determined. While the viabilities of HEK293T cells infected by AAV r3.45/HpNP complexes under magnetic forces were slightly reduced as compared to the negative control (i.e., cells without infection), the metabolic activities of PC12 cells transduced by AAV r3.45/HpNP complexes were comparable to those of cells cultured without viral infection (Fig. 3A and B). AAV r3.45/HpNP delivery with or without magnetic forces resulted in similar trends of cell viability, indicating that magnetic exposure did not influence cellular metabolic activity. Interestingly, for HEK293T cells, the highest quantity of nanoparticles (10 μg) under the longest magnetic exposure (180 min) induced a significant reduction in cell viabilities compared to the other conditions, possibly due to the

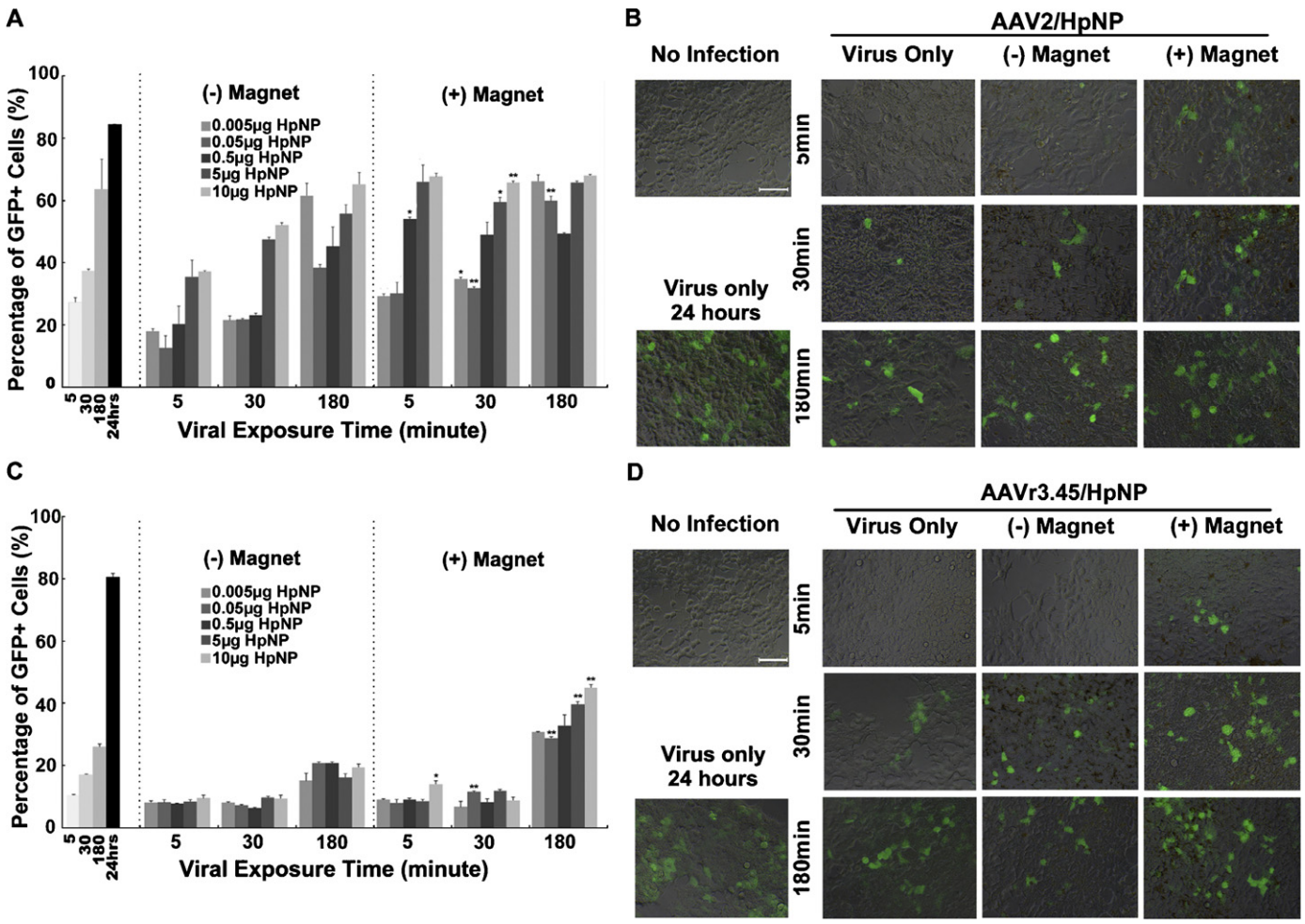

Fig. 4. Cellular transduction of HEK293T cells by AAV2/HpNPs (A), (B) and by AAV r3.45/HpNP complexes (C), (D) The percentage of GFP-positive HEK293T cells due to the delivery of AAV2/HpNPs (A) and AAVr3.45/HpNPs (C) out of the total number of cells at 2 days post-infection. The genomic MOI (i.e., viral genomic particles/cells) was 10^4. Values are reported as mean ± SD. The symbols * and ** indicate statistically differences between infections by AAV2/HpNPs without magnetic forces and the ones (the same NP quantity) with magnetic forces ($P < 0.05$ and $P < 0.01$, respectively). Representative GFP-expressing HEK293T cells due to the delivery of AAV2/HpNPs (10 μg) (B) and AAV r3.45/HpNPs (10 μg) (D). The scale bar indicates 100 μm.

cytotoxicity of the nanoparticle itself or the presence of large numbers of nanoparticles internalized across the cellular membrane (Kamei et al., 2009; Prijic et al., 2010; Song et al., 2010).

3.3. Enhanced cellular transduction by magnetically guided AAV delivery

HpNP-mediated AAV delivery under magnetic forces, especially with larger quantities of nanoparticles, resulted in significantly enhanced cellular transductions in both cell types (HEK293T and PC12) compared with HpNP-mediated delivery without magnetic forces (Figs. 4 and 5). For HEK293T infection with AAV2/HpNPs (genomic MOI: 10^4), a shorter magnet exposure (i.e., 5 and 30 min) with larger quantities of nanoparticles maximized the effect of magnetic guidance of AAV2/HpNP complexes on cellular transduction, which was consistent with previous studies (Fig. 4A and B) (Kamei et al., 2009; Pickard et al., 2011). Interestingly, magnetic exposure of AAV2/HpNP complexes for 180 min (except for 0.05 μg HpNP quantity) did not enhance cellular transduction as compared with freely dispersed AAV2 delivery or non-magnetically guided AAV2/HpNP delivery, presumably due to the complete non-magnetic sedimentation of AAV2 vectors at 180 min-post infection (Plank et al., 2003). Importantly, magnetically guided AAV delivery offered highly localized gene expression in a confined area above the magnet (not shown), possibly implying the distribution of magnetic field exerted on the cells or demonstrating potential applications of magnetically guided gene delivery system, such as for spatial control of gene expression in biological systems (Scherer et al., 2002; Li et al., 2008).

The longest exposure (i.e., 180 min) of AAV r3.45/HpNP complexes in HEK293T infection (genomic MOI: 10^4) demonstrated substantially improved cellular transduction efficiencies compared to both the delivery of virus only and non-magnetically guided AAVr3.45/HpNPs, possibly indicating that forced entry of AAV r3.45 in HEK293T infection played a crucial role for improving cellular transduction (Fig. 4C and D). At shorter viral exposures of AAV r3.45/HpNPs (<30 min), however, a substantial improvement in cellular transduction by the magnetic guidance of AAV r3.45/HpNP complexes as compared with non-magnetic, virus-only delivery was not observed. This result might be caused by the lower binding capacities of AAVr3.45 to HpNPs (33.2–75.4%), such that proportions of AAV r3.45 that were freely dispersed without formulating with HpNPs became high. The reduced binding affinity of AAVr3.45 onto the HpNPs might result in diminished driving forces toward target cells under magnetic fields, ultimately mitigating the dramatic effect of magnetically reinforced gene delivery.

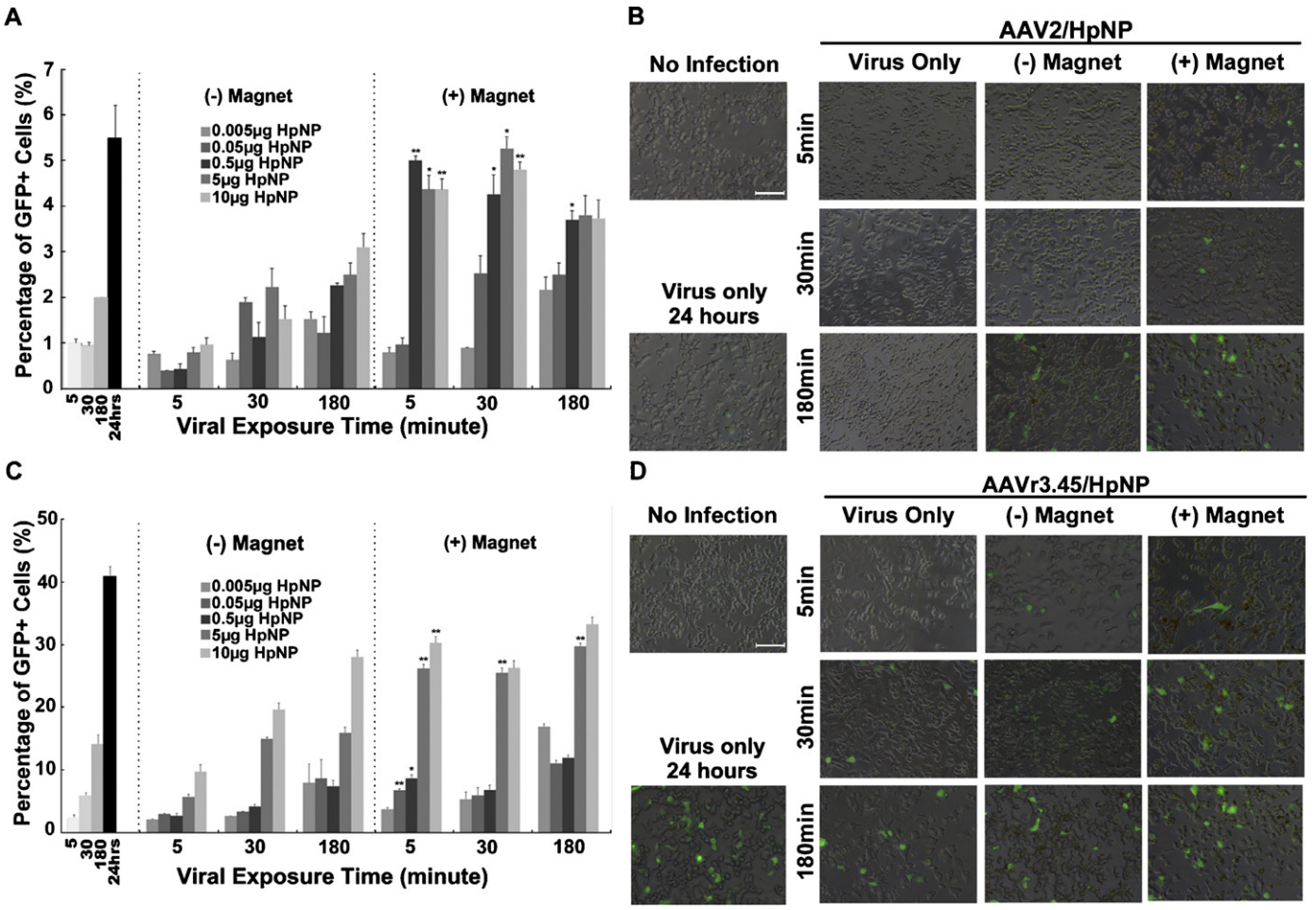

Fig. 5. Cellular transduction of PC12 cells by AAV2/HpNPs (A), (B) and by AAVr3.45/HpNP complexes (C), (D): The percentage of GFP-positive PC12 cells due to the delivery of AAV2/HpNPs (A) and AAVr3.45/HpNPs (C) out of the total number of cells at 2 days post-infection. The genomic MOI (i.e., viral genomic particles/cells) was 10^5. Values are reported as mean ± SD. The symbols * and ** indicate statistically differences between infections by AAV2/HpNPs without magnetic forces and the ones (the same NP quantity) with magnetic forces (the same HpNP quantities) ($P < 0.05$ and $P < 0.01$, respectively). Representative GFP-expressing PC12 cells due to the delivery of AAV2/HpNPs (10 μg) (B) and AAVr3.45/HpNPs (10 μg) (D). The scale bar indicates 100 μm.

Additionally, in HEK293T cell infection, magnetically driven AAV/HpNP complexes induced lower transduction efficiency than conventional transduction, that is, 24-h exposure of viral vectors without magnetic forces prior to medium replacement, possibly because HEK293T is a highly permissive cell type to both wild-type AAV2 and AAVr3.45 (Jang et al., 2011).

In transducing PC12 cells, magnetically guided AAV/HpNP complexes (both AAV2 and AAVr3.45) (genomic MOI: 10^5) led to comparable cellular transduction as compared with the conventional transduction (i.e., 24-h exposure of virus only) (Fig. 5), possibly indicating mechanisms of magnetically guided viral gene delivery may be cell-line specific (Huth et al., 2004). Only 30–180 min-viral exposure under magnetic forces yielded similar transduction to that obtained upon 24 h-incubation of virus in freely dispersed formulation, revealing that magnetic guidance of viral gene delivery can save time to induce sufficient cellular transduction (Fig. 5A and C) (Plank et al., 2003; Haim et al., 2005). Compared with HpNP-mediated AAV delivery without magnetic forces, magnetically guided AAV/HpNP complexes resulted in significantly enhanced cellular transduction, especially with the ones formulated with higher NP quantities (>0.5 μg). As with the HEK293T infection, the effect of magnetic delivery was maximized when PC12 cells were exposed for a short time period (5, 30 min) to AAV vectors (AAV2 and AAV r3.45) complexed with higher quantities of HpNPs (>0.5 μg for AAV2, >5 μg for AAV r3.45), ultimately leading to slightly improved or similar transduction efficiencies compared to those from the 180-min exposure with a larger quantity of HpNPs.

3.4. Internalization of magnetically guided AAV delivery

To investigate the rapid internalization of AAV/HpNP complexes under magnetic forces and the effect of the internalization on cellular transduction, cells (HEK293T, PC12) were exposed to the complexes for designated time points (i.e., 5, 30, or 180 min) and subsequently trypsinized and re-plated onto a fresh dish. Once cells are fully recovered from trypsinization (after approximately 12 h), the presence of fluorescently labeled AAV vectors within cells was visualized.

Upon delivering virus by magnetic guidance, large amounts of fluorescently labeled AAV vectors were observed within the cytoplasm. Furthermore, the quantity of AAV vectors localized within cells gradually increased as viral exposure time increased (Fig. 6). The discrepancy between the quantity of fluorescently labeled AAV vectors present within cells with or without magnetic forces seemed to be significant; however, fluorescently tagged virus was also observed in virus-only formulation and in non-magnetic delivery at the longest viral exposure time (i.e., 180 min).

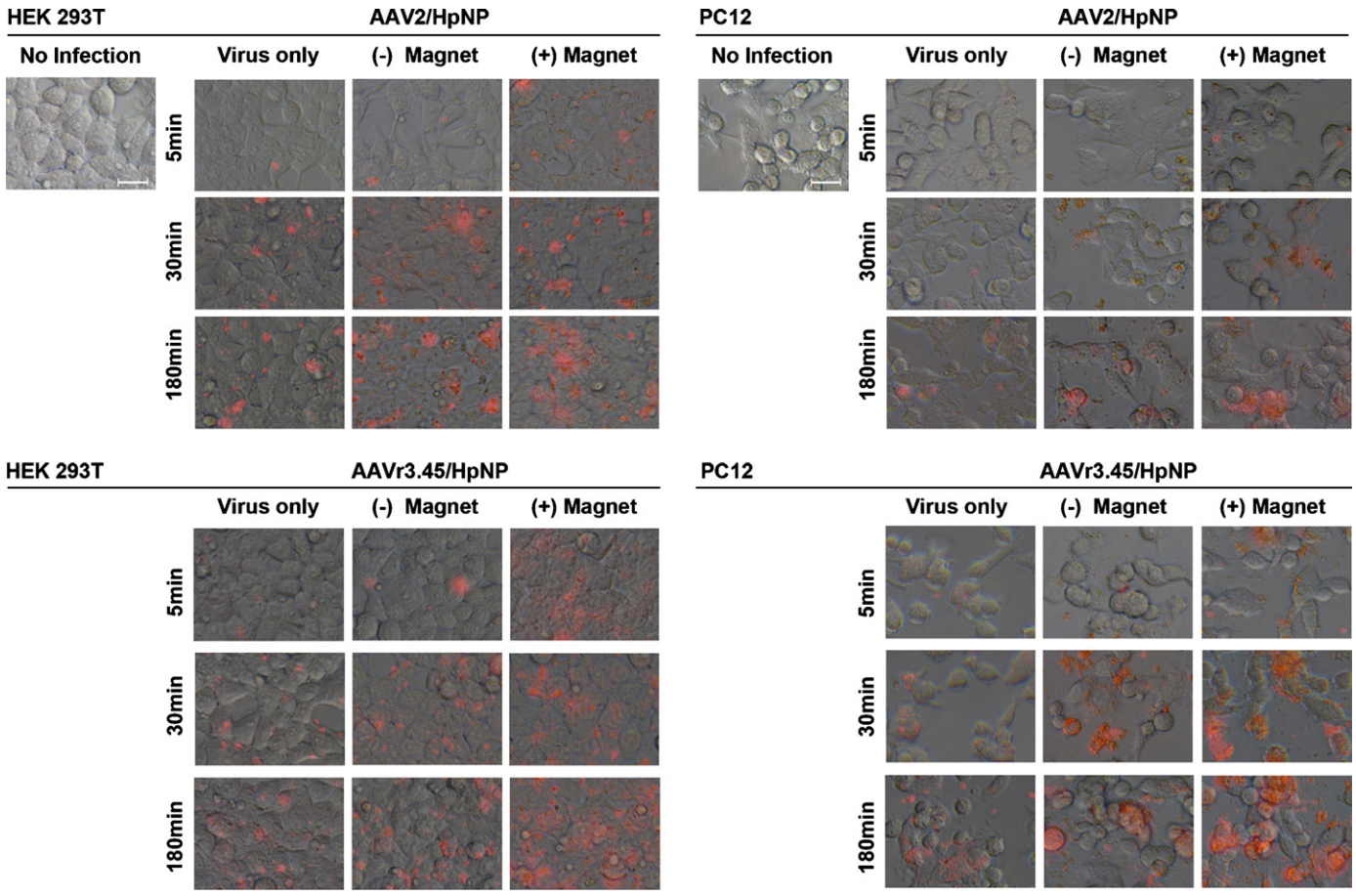

Fig. 6. Internalization of fluorescently labeled AAV vectors. Prior to visualizing the internalization, the cells were exposed at different viral exposures (5, 30, or 180 min), vigorously rinsed with PBS, trypsinized, and re-plated onto fresh 24-well dishes. To visualize the localization of fluorescently labeled virus within the cytoplasm, phase-contrast images of cells and fluorescent images of Alexa-Fluor 594 tagged virus (red color) were overlaid. The scale bar indicates 25 μm. (For interpretation of the references to color in figure legend, the reader is referred to the web version of the article.)

Sufficient non-magnetic sedimentation of viral vectors at the 180 min time point may have caused the reduction in the discrepancy. Our observation may imply that a forced entry of the AAV/HpNP complexes across the cellular membrane under magnetic forces might be a key mechanism of gene delivery during short exposures (<30 min). (Kim et al., 2011) But the coordination between the direct penetration and surface-association of viral vectors could be a major mechanism of gene delivery during longer viral exposures (>180 min).

3.5. Enhanced elongation of neurites by magnetically guided AAV delivery

The rapid internalization of AAV vectors followed by enhanced cellular transduction produced abundant protein that is sufficient to induce physiological responses of PC12, such as neurite extension. Neurite elongation by PC12 was employed to examine physiological responses against functional nerve growth factor (NGF) secreted from PC12 infected by magnetically enhanced AAV delivery. Nerve growth factor (NGF) coding DNA driven by the CMV promoter was packaged into both AAV2 and AAV r3.45. PC12 was then incubated with AAV2/HpNPs or AAV r3.45/HpNPs with or without magnetic forces to induce neurite extension from PC12. Delivery of virus only (AAV-NGF) and NGF protein (100 ng/mL) were utilized as positive controls, and no infection condition was employed as a negative control. The averaged values of total neurite lengths per field at 2 days post-infection were quantified to evaluate neurite extension. The quantity of HpNPs formulated with AAV vectors (i.e., AAV2 and AAV r3.45) was fixed at 10 μg, which yielded the highest GFP expressions in PC12.

A longer magnetic exposure of AAV/HpNP complexes encoding NGF resulted in the gradual increase in neurite extension (Fig. 7). Higher transduction levels by AAV r3.45/HpNPs under magnetic forces produced longer neurites than those generated by AAV2/HpNPs. The lengths of neurite extension from PC12 by 180 min-magnet exposure of AAV r3.45/HpNP complexes were significantly longer (1207.3 ± 405.1 μm) than those obtained by the delivery of AAVr3.45 virus alone (360.3 ± 136.9 μm) or by the incubation with NGF protein (100 ng/mL) (314.0 ± 92.9 μm) ($P < 0.05$) (Fig. 7A). Substantial numbers of neurites were observed upon the longest magnetic exposure (i.e., 180 min) of AAV2 and AAV r3.45 encoding NGF (Fig. 7B). This result demonstrates that enhanced gene delivery mediated by magnetic guidance has the ability to produce sufficient protein to induce a physiological response. Even though transduction efficiencies of PC12 by AAV2/HpNPs under magnetic fields were low (~5%), the 180 min-exposure of AAV2/HpNPs encoding NGF under magnetic forces resulted in significantly increased neurite lengths (838.2 ± 119.6 μm) as compared with the positive control, that is, direct NGF protein delivery (314.0 ± 92.9 μm), revealing a promising benefit of magnetically guided AAV delivery for numerous gene therapy applications.

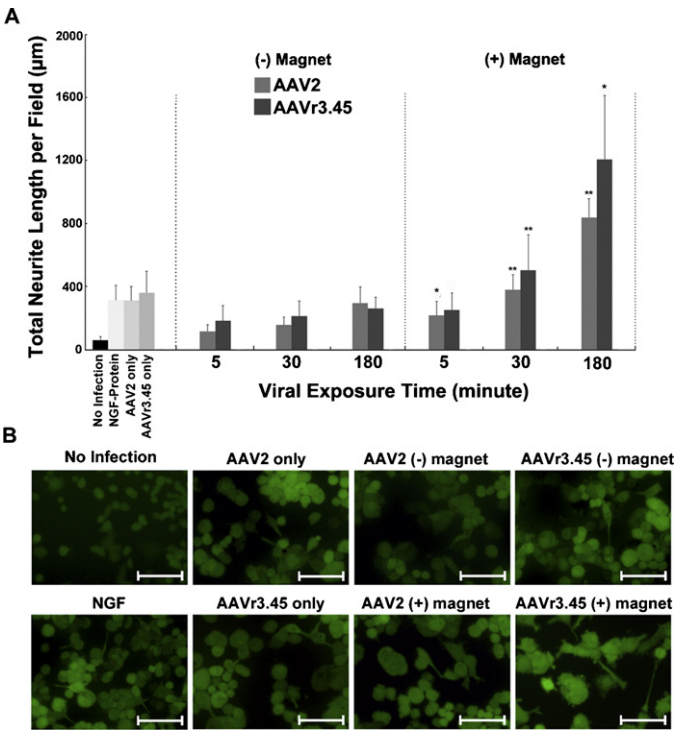

Fig. 7. Neurite outgrowth by PC12 following AAV/HpNP-mediated expression of NGF: (A) total neurite length extended by various exposure times (5, 30, or 180 min) of AAV2-, AAV r3.45 formulated with different quantities of HpNPs with or without magnetic forces. Fifteen random fields of views from three images (triplicate) were chosen, and the total lengths of neuritis were quantified using the tracing algorithm in the Neuron J plug-in for ImageJ. Values are reported as mean ± standard deviation (SD). The symbols *, ** indicate statistical differences compared with neurite lengths extended by AAV/HpNPs delivery without magnetic forces and the ones (the same NP quantity) with magnetic forces (the same HpNP quantities) ($P < 0.05$ and $P < 0.01$, respectively). (B) Representative images demonstrating neurite elongation at 2 days post-infection. Cells were stained using fluorescein diacetate (FDA) for easy recognition of neurite extensions.

4. Conclusions

We report an AAV delivery system capable of highly efficient and rapid cellular transduction by employing magnetic forces. Magnetically guided AAV/HpNP delivery induced rapid internalization and significantly enhanced cellular transduction. Additionally, the rapid and efficient gene delivery approach resulted in the production and secretion of physiological levels of functional growth factor (NGF), which led to robust neurite extension by PC12 as compared to direct growth factor delivery or non-magnetic mediated AAV delivery. The successful establishment of an AAV delivery system with the ability to efficiently and rapidly infect target cells will provide a powerful platform for a variety of gene therapy applications.

Acknowledgements

This work was supported by Advanced Biomass R&D Center (ABC) of Korea (Grant No. 2010-0029734) and National Research Foundation grant funded by the Korea Government (MEST) (No. 2011-0027727).

Author contributions: J.H. Hwang and J.H. Jang designed the experiments and wrote the manuscript. J.H. Jang supervised the study; J.H. Hwang performed the majority of experiments; E.M. Kim performed visualization of internalized viral vectors; S. Lee assisted in the quantification of neurite lengths; and J.S. Kim generated the AAV helper plasmid coding NGF. C.H. Lee and I.S. Ahn provided scientific discussions.

References

Cartier, N., et al., 2009. Hematopoietic stem cell gene therapy with a lentiviral vector in X-linked adrenoleukodystrophy. Science 326, 818–823.
Dobson, J., 2006. Gene therapy progress and prospects: magnetic nanoparticle-based gene delivery. Gene Ther. 13, 283–287.
Fisher, K.J., et al., 1997. Recombinant adeno-associated virus for muscle directed gene therapy. Nat. Med. 3, 306–312.
Flannery, J.G., et al., 1997. Efficient photoreceptor-targeted gene expression in vivo by recombinant adeno-associated virus. Proc. Natl. Acad. Sci. U. S. A. 94, 6916–6921.
Haim., H., et al., 2005. Synchronized infection of cell cultures by magnetically controlled virus. J. Virol. 79, 622–625.
Huth, S., et al., 2004. Insights into the mechanism of magnetofection using PEI-based magnetofectins for gene transfer. J. Gene. Med. 6, 923–936.
Jang, J.H., et al., 2011. An evolved adeno-associated viral variant enhances gene delivery and gene targeting in neural stem cells. Mol. Ther. 19, 667–675.
Kamei, K., et al., 2009. Direct cell entry of gold/iron-oxide magnetic nanoparticles in adenovirus mediated gene delivery. Biomaterials 30, 1809–1814.
Kaplitt, M.G., et al., 1994. Long-term gene expression and phenotypic correction using adeno-associated virus vectors in the mammalian brain. Nat. Genet. 8, 148–154.
Kay, M.A., et al., 2000. Evidence for gene transfer and expression of factor IX in haemophilia B patients treated with an AAV vector. Nat. Genet. 24, 257–261.
Kim, E., et al., 2011. Magnetically enhanced adeno-associated viral vector delivery for human neural stem cell infection. Biomaterials 32, 8654–8662.
Koerber, J.T., et al., 2006. Construction of diverse adeno-associated viral libraries for directed evolution of enhanced gene delivery vehicles. Nat. Protoc. 1, 701–706.
Li, W., et al., 2008. Enhanced thoracic gene delivery by magnetic nanobead-mediated vector. J. Gene Med. 10, 897–909.
Lin., M.M., et al., 2008. Development of superparamagnetic iron oxide nanoparticles (SPIONS) for translation to clinical applications. IEEE Trans. Nanobioscience 7, 298–305.
Maguire, A.M., et al., 2009. Age-dependent effects of RPE65 gene therapy for Leber's congenital amaurosis: a phase 1 dose-escalation trial. Lancet 374, 1597–1605.
Maheshri, N., et al., 2006. Directed evolution of adeno-associated virus yields enhanced gene delivery vectors. Nat. Biotechnol. 24, 198–204.
Meijering, E., et al., 2004. Design and validation of a tool for neurite tracing and analysis in fluorescence microscopy images. Cytometry A 58, 167–176.
Orlando, C., et al., 2010. Magnetically guided lentiviral-mediated transduction of airway epithelial cells. J. Gene Med. 12, 747–754.
Pickard, M.R., et al., 2011. The transfection of multipotent neural precursor/stem cell transplant populations with magnetic nanoparticles. Biomaterials 32, 2274–2284.
Plank, C., et al., 2003. The magnetofection method: using magnetic force to enhance gene delivery. Biol. Chem. 384, 737–747.
Prijic, S., et al., 2010. Increased cellular uptake of biocompatible superparamagnetic iron oxide nanoparticles into malignant cells by an external magnetic field. J. Membr. Biol. 236, 167–179.
Scherer, F., et al., 2002. Magnetofection: enhancing and targeting gene delivery by magnetic force in vitro and in vivo. Gene Ther. 9, 102–109.
Selkirk, S.M., 2004. Gene therapy in clinical medicine. Postgrad. Med. J. 80, 560–570.
Smith-Arica, J.R., et al., 2003. Infection efficiency of human and mouse embryonic stem cells using adenoviral and adeno-associated viral vectors. Cloning Stem Cells 5, 51–62.
Song., H.P., et al., 2010. Gene transfer using self-assembled ternary complexes of cationic magnetic nanoparticles, plasmid DNA and cell-penetrating Tat peptide. Biomaterials 31, 769–778.
Zolotukhin, S., et al., 1999. Recombinant adeno-associated virus purification using novel methods improves infectious titer and yield. Gene Ther. 6, 973–985.